Analyses of queen Hetepheres' bracelets from her celebrated tomb in Giza reveals new information on silver, metallurgy and trade in Old Kingdom Egypt, c. 2600 BC

Karin Sowada, Richard Newman, Francis Albarède, Gillan Davis, Michele R Derrick, Timothy D Murphy, Damian B Gore

Journal of Archaeological Science: Reports 49 (2023) 103978

Contents lists available at ScienceDirect

Journal of Archaeological Science: Reports

journal homepage: www.elsevier.com/locate/jasrep

Analyses of queen Hetepheres' bracelets from her celebrated tomb in Giza reveals new information on silver, metallurgy and trade in Old Kingdom Egypt, c. 2600 BC

Karin Sowada [a,*], Richard Newman [b], Francis Albarède [c], Gillan Davis [d], Michele R. Derrick [b], Timothy D. Murphy [e,f], Damian B. Gore [f]

[a] Department of History and Archaeology, Macquarie University, Sydney, Australia
[b] Museum of Fine Arts, Boston, United States of America
[c] Ecole Normale Supérieure de Lyon, France
[d] Australian Catholic University, Sydney, Australia
[e] School of Natural Sciences, Macquarie University, Sydney, Australia
[f] Newspec Pty Ltd, Myrtle Bank, Australia

ARTICLE INFO

Keywords:
Egypt
Old Kingdom
Trade
Silver
Metallurgy
Elemental composition
Lead isotopes

ABSTRACT

Egypt has no domestic silver ore sources and silver is rarely found in the Egyptian archaeological record until the Middle Bronze Age. Bracelets found in the tomb of queen Hetepheres I, mother of pyramid builder king Khufu (date of reign c. 2589–2566 BC), form the largest and most famous collection of silver artefacts from early Egypt, but they have not been analysed for decades. We analysed samples from the collection in the Museum of Fine Arts, Boston using bulk XRF, micro-XRF, SEM-EDS, X-ray diffractometry and MC-ICP-MS to obtain elemental and mineralogical compositions and lead isotope ratios, to understand the nature and metallurgical treatment of the metal and identify the possible ore source. We found that the pieces consist of silver with trace copper, gold, lead and other elements. The minerals are silver, silver chloride and a possible trace of copper chloride. Surprisingly, the lead isotope ratios are consistent with ores from the Cyclades (Aegean islands, Greece), and to a lesser extent from Lavrion (Attica, Greece), and not partitioned from gold or electrum as previously surmised. Sources in Anatolia (Western Asia) can be excluded with a high degree of confidence. Imaging of a cross-section of a bracelet fragment reveals that the metal was repeatedly annealed and cold-hammered during creation of the artefacts. The results provide new information about silver ore sources, commodity exchange networks and metallurgy in Egypt during the Early Bronze Age.

1. Introduction

Celebrated among Old Kingdom Egyptian silver objects are the bracelets of queen Hetepheres I (c. 2600 BC), mother of king Khufu, builder of the Great Pyramid at Giza (date of reign c. 2589–2566 BC, Shaw, 2000: 482). The rarity of these objects is threefold: surviving royal burial deposits from this period are rare; only small quantities of silver survived in the archaeological record until the Middle Bronze Age (c. 1900 BC); and Egypt lacks silver ore deposits. Few silver artefacts from the Old Kingdom have been analysed.

Silver (Ag) artefacts first appeared in Egypt during the 4th millennium BC but the original source then, and in the 3rd millennium, is unknown (Ogden, 2000: 170; Hauptmann and von Bohlen, 2011). Ancient Egyptian texts do not mention any local sources (Gale and Stos-Gale, 1981: 104), but an older view, derived from the presence of gold (Au) in Ag objects, plus the high Ag content of Egyptian gold and electrum, holds that Ag was derived from local sources (Mishara and Meyers, 1974; Lucas and Harris, 1962: 248; Gale and Stos-Gale, 1981: 113; Ogden 2000: 170–71). An alternative view is that Ag was imported to Egypt, possibly via Byblos on the Lebanese coast, owing to many Ag objects found in Byblos tombs from the late fourth millennium (Prag, 1986: 38). Exchange mechanisms between Egypt and Lebanon are attested from the Naqada IIIA1 period (c. 3320 BC) and probably earlier (Hartung, 2001; Hartung et al., 2015; Ownby et al., 2022). Over the ensuing centuries, Egypt developed intensive trade relations with Byblos and the region. By the 4th Dynasty, the Egyptian state also sourced

* Corresponding author. Address: Department of History and Archaeology, Level 1 25WW, Macquarie University, NSW 2109, Sydney, Australia.
E-mail address: karin.sowada@mq.edu.au (K. Sowada).

https://doi.org/10.1016/j.jasrep.2023.103978
Received 8 October 2022; Received in revised form 13 March 2023; Accepted 17 March 2023
Available online 1 May 2023

commodities directly or through intermediaries, down-the-line and indirect networks (Sowada, 2009: 245–55). By the late Old Kingdom (c. 2300 BC), networks for metals extended eastward, accessing silver from Ebla (Marcolin and Diego Espinel 2011; Biga and Steinkeller 2021).

The tomb of queen Hetepheres I (Tomb G 7000X) was discovered at Giza in 1925 by the Harvard University–Museum of Fine Arts (MFA) Joint Expedition (Reisner, 1927). Hetepheres was one of Egypt's most important queens: wife of 4th Dynasty king Sneferu and mother of Khufu, the greatest builders of the Old Kingdom (c. 2686–2180 BC). Her intact sepulchre is the richest known from the period, with many treasures including gilded furniture, gold vessels and jewellery (Harvard, 2023). The bracelets were found surrounded by the remains of a wooden box covered with gold sheeting, bearing the hieroglyphic inscription 'Box containing *deben*-rings' (Reisner, 1927: 21) (Fig. 1A). Twenty *deben*-rings or bracelets were originally interred, one set of ten for each limb, originally packed inside the box (Reisner and Smith, 1955: 43–44, Figs 44; Plates 36–37). Recovered in different states of preservation, most were sent to the Egyptian Museum (Cairo JE53271–3) (Fig. 1B), and two others, plus many fragments, were gifted to the Museum of Fine Arts (MFA) in Boston in 1947 by the Egyptian Government (MFA 47.1699–1702) (Reisner and Smith, 1955: 20, 43–44, pl. 38; Aldred, 1971: 33, 133, 158, 175, Pl. 3; Ziegler, 1999: 20–21). The bracelets on display at the MFA are fragmentary (Fig. 1C, right) with additional unattached loose pieces kept in climate-controlled storage (MFA 47.1702) (Fig. 2A).

The bracelets, made of a metal rare to Egypt, are a statement of royal privilege and taste. The thin metal worked into a crescent shape and the use of turquoise, lapis lazuli and carnelian inlay, stylistically mark the bracelets as made in Egypt and not elsewhere (Petrie, 1901:Pl. ix.4; Aldred, 1971: 33-4, pl. 13). Each ring is of diminishing size, made from a thin metal sheet formed around a convex core, creating a hollow cavity on the underside. Depressions impressed into the exterior received stone inlays forming the shape of butterflies. At least four insects are depicted on each bracelet, rendered using small pieces of turquoise, carnelian and lapis lazuli, with each butterfly separated by a circular piece of carnelian. In several places, pieces of real lapis have been substituted by painted plaster (Reisner and Smith, 1955: 44).

The metal was examined nearly 100 years ago by A. Lucas and H.E. Cox and found to be 90.1% Ag, 8.9% Au and 1.0% copper (Cu) (Reisner, 1928; Reisner and Smith, 1955: 44). The location(s) measured, and the method of analysis, were not reported. They noted visible 'yellow patches on the surface … due to the unequal distribution of the gold present' (Lucas and Harris, 1962: 246, 248). Lucas (1962: 249) also noted that silver objects 'with a very much lower gold content … may have been imported as early as the Old Kingdom at least'. Since then, the MFA bracelets have not been analysed. Our research presents new images, and elemental, mineralogical and lead isotope analyses, helping to characterise the metal composition, and constrain the provenance of the Ag and method of manufacture of these unique objects.

2. Materials and methods

2.1. Description

The artefacts on exhibition at the MFA could not be sampled, however three small bags (B1-B3) of corroded bracelet fragments were available for study (Fig. 2). A piece from bag B2 was metallic in appearance (MFA 47.1702 B2P1, Fig. 2C–D) (hereafter "B2P1"), while the remaining pieces were heavily corroded. A sample of metallic fragment MFA 47.1702 B2P1, and corroded fragment MFA 47.1702 B1P4 (Fig. 2A centre left, and 2B) (hereafter "B1P4"), were selected for further study.

2.2. Elemental composition

Bulk XRF. Elemental compositions were measured from five locations on the corrosion-free metal forming fragment B2P1, using a Bruker Artax X-ray fluorescence spectrometer (XRF) with rhodium (Rh) anode tube operated at 40 kV, 400 μA, 60 s live time, a 0.65 mm collimator, no filter and all measurements were made in air. Based on counting statistics, limits of detection for elements was estimated to be 0.1 wt% for iron (Fe), Cu and lead (Pb), and 0.3 wt% for Ag and Au. Quantitative results were determined by Bruker software using one laboratory Ag standard. Based on previous experience, accuracy for Ag and Au was estimated as ±1 wt% for Cu and ±0.1 wt% for Pb.

The bulk elemental compositions of ~1.4 g of corrosion products of fragment B1P4 were measured using a Panalytical Epsilon 3 benchtop energy dispersive X-ray fluorescence spectrometer, with rhodium (Rh) anode tube and a 6 mm ellipse measurement area. Measurement conditions were 50 kV, 60 s, Ag filter; 50 kV, 300 μm Cu filter, 60 s; 20 kV, 200 μm Al filter, 60 s; 12 kV, 50 μm Al filter, 100 s; 5 kV, no filter, 100 s and all measurements were made in air. Limits of detection for elements was estimated to be 0.001 wt% for iron (Fe), Cu and lead (Pb), and 0.005 wt% for Au. Quantitative results were determined using the Panalytical Omnian software, trained using a range of MBH reference materials consisting of trace elements in Ag matrices. Accuracies for Fe, Cu and Pb were better than 10% for concentrations >0.1 wt%. Data reduction and quantification were carried out in the Epsilon 3 software version 1.1. Data were summed to 100%.

Micro-XRF. Elemental maps were produced from a ~9.1 × 6.8 mm

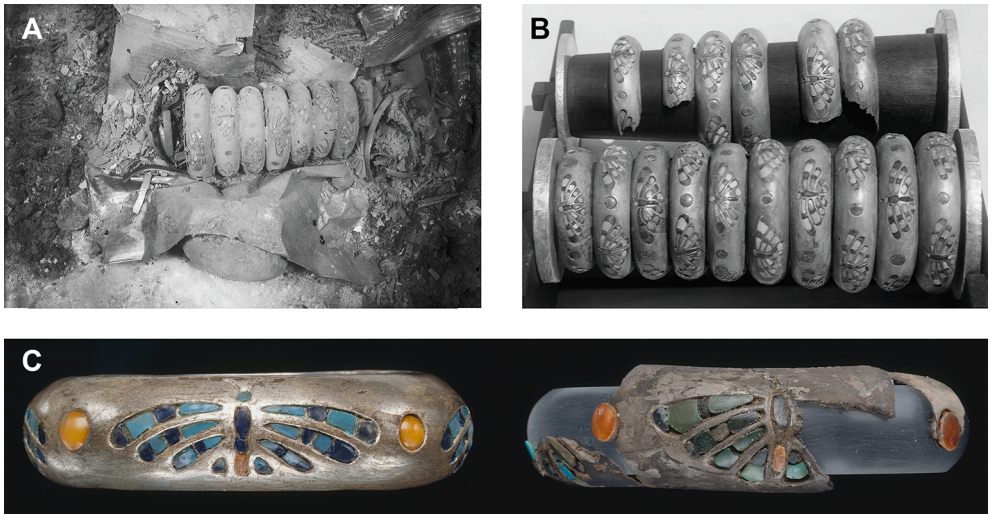

Fig. 1. (A) Bracelets in the burial chamber of Tomb G 7000X as discovered by George Reisner in 1925 (Photographer: Mustapha Abu el-Hamd, August 25 1926) (B) Bracelets in restored frame, Cairo JE 53271–3 (Photographer: Mohammedani Ibrahim, August 11 1929) (C) A bracelet (right) in the Museum of Fine Arts, Boston, MFA 47.1700. The bracelet on the left is an electrotype reproduction made in 1947, MFA 52.1837 (Harvard University—Boston Museum of Fine Arts Expedition; All Photographs © April 2023 Museum of Fine Arts, Boston).

Fig. 2. (A) Bag B1 of corroded bracelet fragments in the Museum of Fine Arts, Boston, MFA 47.1702. MFA 47.1702 B1P4 shown second from left, centre (Photograph © April 2023 Museum of Fine Arts, Boston) (B) Detail of MFA 47.1702 B1P4 (C–D) Metallic fragment recto (left) and verso (right) MFA 47.1702 B2P1 (Photograph K. Sowada, © April 2023 Museum of Fine Arts, Boston).

piece of corrosion product B1P4, using a Bruker M4 Tornado with Rh anode tube operated at 50 kV, 200 μA, twin X'Flash 30 detectors and measurement conditions of 20 μm spot size, with a dwell time of 20 ms/pixel, in vacuum. Elemental compositions of each pixel, or user-definable areas, can be quantified independently. Spectra were quantified using fundamental parameters calibrated using pure element standards; the X'Flash detectors were calibrated using manganese (99.99%) and zirconium (99.99%) reference materials supplied by Bruker.

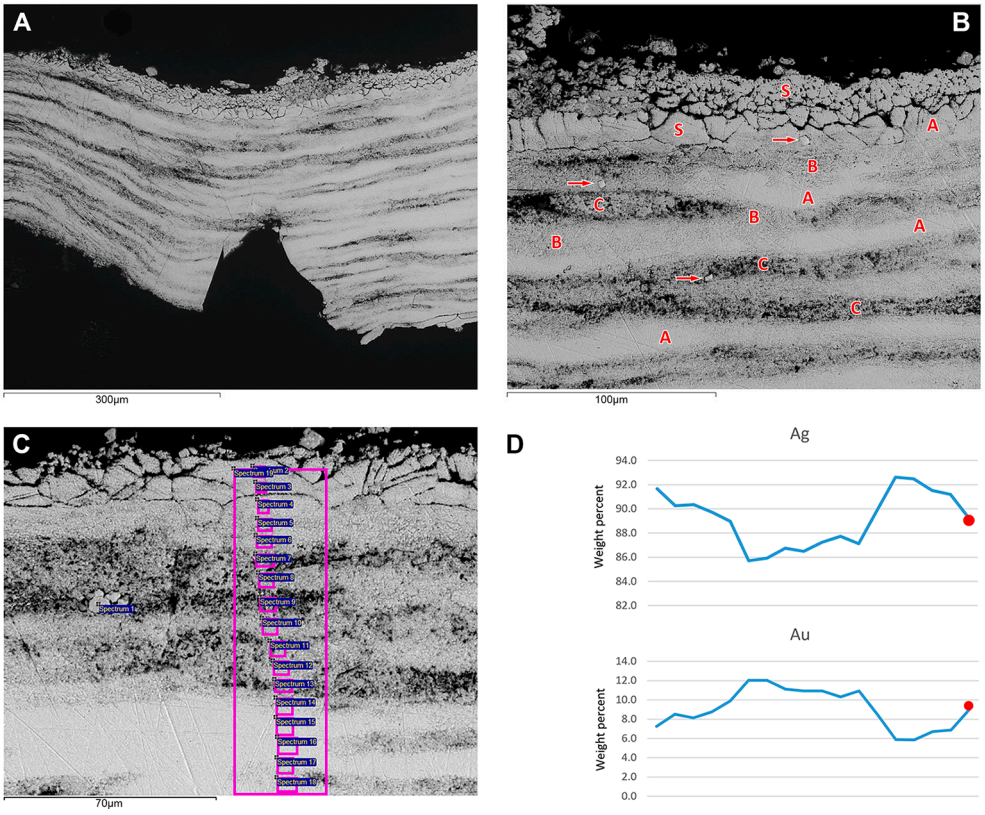

Fig. 3. (A) Back-scattered electron image of part of the polished cross section from MFA 47.1702 B2P1 (B) Detail from image A at higher magnification, showing the metal structure to consist of elongated islands of uncorroded Ag metal ("A") intercalated with a more porous matrix ("B") transitioning to an open framework of corroded metal ("C"). (Images R. Newman, © Museum of Fine Arts, Boston) (C) Concentrations of Ag and Au in small regions (purple outlines) were determined and plotted in (D). The plots begin at the top of the area shown in (C) and end at the bottom. The final data point is for the larger rectangular area and can be considered the average for this part of the sample (about 89% Ag and 9% Au). Note that Au has higher concentrations and Ag lower in the more heavily corroded areas (data points in the middle of the plots).

Calibrations were verified using stainless steel. Limits of detection for the elements reported are ~40 mg/kg.

SEM-EDS. A small solid sample was taken from B2P1 and embedded in Buehler EpoThin epoxy resin and prepared as a polished section. This sample was examined using a JEOL JSM-6460LV scanning electron microscope with energy dispersive spectrometry (SEM-EDS). Operating conditions were 35 Pa chamber pressure, 20 kV with ~1nA beam current. The working distance was 10 mm and quantitative elemental analyses were collected over 10 s live time. An 80 mm^2 Oxford X-Max^N silicon drift detector was used with Oxford default standards and Oxford Instruments INCA software. Quantitative SEM-EDS results utilized pure metal standards, with matrix corrections carried out in the INCA software. Limits of detection, estimated from counting statistics, are 0.1 wt % for Cu, 0.2 wt% for Ag and Au, 0.3 wt% for Pb. Accuracy is estimated to be +/-2% (relative) for Ag and Au, +/-10% (relative) for the other elements. Since the beam current was not monitored during analyses, all results were normalized. Back-scattered electron images of the section are shown in Fig. 3, with other details in Tables 3 and 4. Numerous point and small area analyses were carried out to determine the alloy composition and the nature of several inclusions found in the metal.

Because analyses were carried out in low vacuum conditions, some oxygen was present in the SEM chamber, and thus oxygen was excluded from the analytical results. Comparison of the relative height of the oxygen peak in the sample spectra with the relative height of the oxygen peak elsewhere on the sample holder indicates that oxygen was at most a very minor component of any of the areas analysed in the section – with the exception of the small antimony (Sb)-containing inclusions, in which the oxygen peak was substantially larger and consequently must be a component of these inclusions.

2.3. Mineralogy

A ~200 mg sample of powder corrosion product from B1P4 was placed on a silicon-crystal low background holder for mineralogical analysis. X-ray diffractograms were collected from 5 to 95° 2θ with a Malvern Panalytical Aeris diffractometer, using tube conditions of 40 kV, 15 mA, cobalt K_α radiation, Pixel-3D detector, Bragg Brentano geometry, and a slew rate of 13° 2θ per minute. Diffractometer calibration and performance was measured using a single silicon crystal. Limits of detection vary from 0.1 to ~2 wt% depending on the crystallinity of the phase. Identification of minerals was conducted using Panalytical's Highscore Plus software v2.2.4, with ICDD PDF2 and PAN-ICSD databases.

2.4. Isotopic analyses

Lead (Pb) isotopic ratios were measured using Multicollector-Inductively Coupled Plasma-Mass Spectrometry (MC-ICP-MS) on sample B2P1. The Pb composition was measured using the Nu Plasma 500 MC-ICP-MS at the Laboratoire de Géologie de Lyon (LGL), Ecole Normale Supérieure de Lyon. Owing to the sample size, only one Pb measurement was possible. Details of the methods and analytical accuracy are outlined in Milot et al. (2021).

3. Results

3.1. Description

Corrosion products were dark grey and retained some shape of the original artefact surface. Granularity or heterogeneity was not readily apparent, but lath-like crystals ~0.5 mm long were visible on the sample surface. The metal in the section was 0.3 to 0.4 mm thick.

3.2. Elemental composition

Bulk XRF. The elemental composition of the ~1.4 g bulk sample of corrosion products in Bag 1 consisted mainly of Ag, with (in decreasing abundance) Au, Cu and Pb (Table 1). Elements likely to be derived from the environment were mainly chlorine (Cl) and calcium (Ca), with smaller amounts of silicon (Si), bromine (Br) and strontium (Sr) (Table 1; B1P4). Following subtraction of those environmental elements and normalization to 100%, the sample consisted of Ag (98 wt%), Au (1 wt%), minor Cu (0.4 wt%) and trace Pb (0.04 wt%) (Table 1; B1P4 corrected). Compared with the bulk corrosion products from B1P4, the compositions of the five selected grains measured from metallic fragment B2P1 were lower in Ag (86–90 wt%) but richer in Au (9–13 wt%) and Pb (0.2–0.3 wt%) than the B1P4 material. Copper was similar between the corrosion products (0.4 wt%) and the five selected grains (0.3–0.6 wt%).

Micro-XRF. The grain taken from sample B1P4 was dominantly Ag (Table 2, Fig. S1). Side 1 was 99% Ag, whereas Side 2 is 86% Ag with the balance consisting dominantly of Au, minor Cu and trace Pb (Table 2, Fig. S2). Uncorrected data from Side 2 show Ca from <1 to 46%, corresponding with light coloured areas on the sample.

SEM-EDS. Analyses of 18 relatively large regions extended over the whole section of B2P1 (Fig. 3C). The average Au content of these regions (which included islands and corroded regions) was about 7%, with around 1% Cu. A small amount of Pb is probably also present (likely <0.5%) but this is difficult to determine accurately from the SEM-EDS analyses.

3.3. Mineralogy

Metallic sample B1P4 consisted dominantly of chlorargyrite (AgCl), with lesser amounts of zero valent silver (Ag) or gold (Au), and possibly small amounts of nantokite (CuCl). Most of the crystallinity is dominated by AgCl (Fig. S3). There were no strong unmatched lines, with only two minor peaks reflecting the presence of a small amount of other minerals whose identity could not be resolved (Fig. S3).

Table 1
Bulk elemental compositions of fragments and corrosion products from silver bracelet MFA 47.1702. Elemental compositions of corrosion products from sample B1P4 were measured using the Panalytical Epsilon 3 XRF (coded "P"); the compositions of five locations on sample B2P1 were measured using the Bruker Artax XRF (coded "B"). "Raw" refers to uncorrected data; "Corr" refers to environmental or surface contaminants (Si, Cl, Ca, Fe, Sr) having been removed and the data corrected (normalized) to 100%. All data in wt%.

Analysis	Si (%)	Cl (%)	Ca (%)	Fe (%)	Cu (%)	Br (%)	Sr (%)	Ag (%)	Au (%)	Pb (%)	Sum (%)
Bulk B1P4 (P Raw)	0.32	17.5	7.64	0.063	0.33	0.021	0.036	73.1	0.90	0.032	99.9
Bulk B1P4 (P Corr)	—	—	—	—	0.45	—	—	98.4	1.21	0.043	100
B2P1_1 (B Corr)	—	—	—	<0.1	0.43	—	—	86.8	12.5	0.26	100
B2P1_2 (B Corr)	—	—	—	<0.1	0.40	—	—	86.4	12.8	0.35	100
B2P1_3 (B Corr)	—	—	—	<0.1	0.56	—	—	88.8	10.3	0.32	100
B2P1_4 (B Corr)	—	—	—	<0.1	0.61	—	—	89.8	9.33	0.19	100
B2P1_5 (B Corr)	—	—	—	<0.1	0.33	—	—	89.0	10.4	0.25	100
B2P1 Corr average				**<0.1**	**0.47**			**88.2**	**11.1**	**0.27**	

Table 2
Micro-XRF measurements of three 0.5 × 0.7 mm areas across the central surface of each side (S1 = Side 1, S2 = Side 2) of a grain taken from sample B1P4 (Fig. S1). All data in wt%.

Analysis	Si (%)	Cl (%)	Ca (%)	Fe (%)	Cu (%)	Sr (%)	Ag (%)	Au (%)	Pb (%)	Sum (%)
S1_1 Raw	0.85	15.0	3.17	0.07	0.02	0.05	76.8	0.05	0.04	96.4
S1_2 Raw	0.61	14.4	9.70	0.06	0.07	0.04	71.6	0.06	0.04	96.9
S1_3 Raw	0.26	3.28	53.8	0.02	0.84	0.04	38.2	0.43	—	97.7
S1_1 Corr	—	—	—	—	0.03	—	99.9	0.06	0.05	100
S1_2 Corr	—	—	—	—	0.09	—	99.8	0.08	0.06	100
S1_3 Corr	—	—	—	—	2.13	—	96.8	1.09	—	100
Corr average					**0.75**		**98.8**	**0.41**	**0.04**	
S2_1 Raw	—	5.30	46.2	0.01	0.22	0.15	47.7	0.28	0.16	100
S2_2 Raw	3.82	13.0	0.07	0.03	2.41	0.00	65.2	15.5	—	100
S2_3 Raw	3.47	8.78	15.6	0.15	5.00	0.06	57.8	9.15	—	100
S2_1 Corr	—	—	—	—	0.45	—	98.6	0.58	0.33	100
S2_2 Corr	—	—	—	—	2.90	—	78.4	18.7	—	100
S2_3 Corr	—	—	—	—	6.93	—	80.4	12.7	—	100
Corr average					**3.43**		**85.7**	**10.7**	**0.11**	

4. Isotopic analyses

Pb isotope abundances were measured in sample B2P1 (Table 5).

5. Discussion

Bulk XRF analyses show that the Hetepheres bracelets are dominantly Ag, with Au, Cu and trace Pb. The elemental compositions of different samples were analysed using four instruments (Bruker Artax XRF, Panalytical Epsilon 3 XRF, Bruker M4 Tornado micro-XRF and JEOL SEM) (Tables 1-4; Table S1); the data are consistent in the major compositions of Ag, Au and Cu and trace Pb forming the sample. However, differences in measurements both within and between methods, result from differences between the samples measured, heterogeneity of each sample, location of the analyses on that sample, and the analytical volume and mass. Bulk analyses, with environmental elements (Si, Cl, Ca etc) subtracted and normalized to 100% give the analyses most representative of the bulk material.

The micro-XRF used in mapping mode revealed the heterogeneity of sample B1P4. Some elements, including Cl and Ag (Fig. S3) appeared uniform in the elemental maps, consistent with their presence as dominant components of the surface of this corroded Ag metal. Elements with heterogeneous distributions are also of interest. Calcium appears in laterally continuous areas around the surface of the piece examined (Figs S1, S2). It appears integral with the corrosion products, but the source of Ca cannot be from the Ag. We consider it to be a surface contaminant, and it will not be discussed further. Some other elements, particularly Fe, are scattered across the surface of the sample (Figs S1, S2) probably representing small grains of iron oxides trapped in the porous matrix of the sample. For this reason, Fe was subtracted from the corrected data in Tables 2 and 3.

Gold, Cu and to lesser concentrations Zn, co-occur on both sides of the piece of sample B1P4 (Figs S1, S2), consistent with the observations of Lucas (1962). This relationship is seen most strikingly on Side 2, where along the left edge, Cu, Zn and Au show the same spatial distribution. Pb is only present at low concentrations overall, and in small grains in the centre and lower side of Side 1 (Fig. S1).

SEM photomicrographs show dark layers parallel to the surface that are characteristic of heavily cold worked metal (Fig. 3). The best local parallels for this technique are known from worked copper of the Early Dynastic Period and the Old Kingdom (Kmošek et al., 2018, Fig. 3). In the case of this bracelet fragment, the metal would have been hammered to flatten it into a thin sheet, accompanied by frequent annealing to prevent embrittlement. Thorough annealing would have recrystallized the entire thickness of metal, but the layered appearance of this sample indicates that annealing was not complete, and there were stressed regions that were more susceptible to corrosion than surrounding recrystallized regions. Higher magnification reveals the metal structure to consist of elongated islands of uncorroded Ag metal, some of which are labelled “A” on the image (Fig. 3B). They are surrounded and separated

Table 3
SEM-EDS elemental analyses of 18 regions (~100 μm × 100 μm) of sample B2P1 across the entire section (each cluster of 4–5 regions falls within parts A-D). The sum of the five reported elements was normalized to 100%. All data in wt%.

Analysis	Cl (wt%)	Cu (wt%)	Ag (wt%)	Au (wt%)	Pb (wt%)	Ag/Au	Cu + Ag + Au + Pb (wt%)
1. Spectrum A1	1.0	0.8	86.6	11.2	0.5	7.7	99.1
2. Spectrum A2	1.9	0.8	85.5	11.3	0.6	7.6	98.2
3. Spectrum A3	1.5	0.9	86.1	10.8	0.7	8.0	98.5
4. Spectrum A4	0.6	0.9	88.5	9.8	0.3	9.0	99.5
5. Spectrum A5	0.5	0.9	90.0	8.2	0.4	11.0	99.5
6. Spectrum B1	0.8	1.0	89.1	8.7	0.5	10.2	99.3
7. Spectrum B2	0.7	0.9	89.5	8.8	0.2	10.2	99.4
8. Spectrum B3	0.7	1.0	89.8	8.2	0.3	11.0	99.3
9. Spectrum B4	0.5	0.8	90.6	7.6	0.5	11.9	99.5
10. Spectrum B5	0.5	1.0	90.1	8.0	0.4	11.3	99.5
11. Spectrum C1	0.5	0.9	90.4	7.8	0.4	11.6	99.5
12. Spectrum C2	0.5	1.0	91.1	7.1	0.3	12.8	99.5
13. Spectrum C3	1.1	0.9	90.8	7.0	0.3	13.0	99.0
14. Spectrum C4	0.4	1.0	89.7	8.4	0.6	10.7	99.7
15. Spectrum D1	0.7	0.9	91.7	6.4	0.4	14.3	99.4
16. Spectrum D2	0.5	0.8	92.0	6.3	0.4	14.6	99.5
17. Spectrum D3	0.5	0.9	91.6	6.8	0.3	13.5	99.6
18. Spectrum D4	1.5	1.1	90.5	6.6	0.3	13.7	98.5
Average	**0.7**	**0.9**	**91.0**	**7.1**	**0.4**	**13.0**	**99.3**

Table 4
SEM-EDS analyses of five inclusions within sample B2P1. Elements are reported as atomic % and summed to 100%. Inclusions 1–4 in the accompanying images also contain oxygen, which was not included in the calculations. Where zinc (Zn) and tin (Sn) were below limits of detection (~0.1%), the value used for averaging was 0.5LOQ (0.5%).

Analysis	Cl (%)	Fe (%)	Ni (%)	Cu (%)	Zn (%)	Ag (%)	Sn (%)	Sb (%)	Au (%)	Pb (%)	Ag/Au
Inclusion 1	2.7	3.2	1.9	0.4	<0.1	31.2	<0.1	28.6	1.6	30.3	19.5
Inclusion 2	0.6	0.2	1.3	0.5	<0.1	18.4	<0.1	30.1	1.6	47.4	11.5
Inclusion 3	0.7	0.3	1.1	0.3	<0.1	23.1	<0.1	29.7	1.7	43.3	13.6
Inclusion 4a	0.8	1.6	1.4	0.7	<0.1	25.7	0.5	23.7	1.9	43.8	13.5
Inclusion 4b	1.2	1.6	2.6	0.3	<0.1	24.4	3.4	25.9	1.5	39.1	16.3
Inclusion 5	0.8	6.9	15.9	6.3	3.8	33.3	1.2	18.2	3.3	10.3	10.1
Average	**1.1**	**2.3**	**4.0**	**1.4**	**0.7**	**26.0**	**0.9**	**26.0**	**1.9**	**35.7**	**14.1**

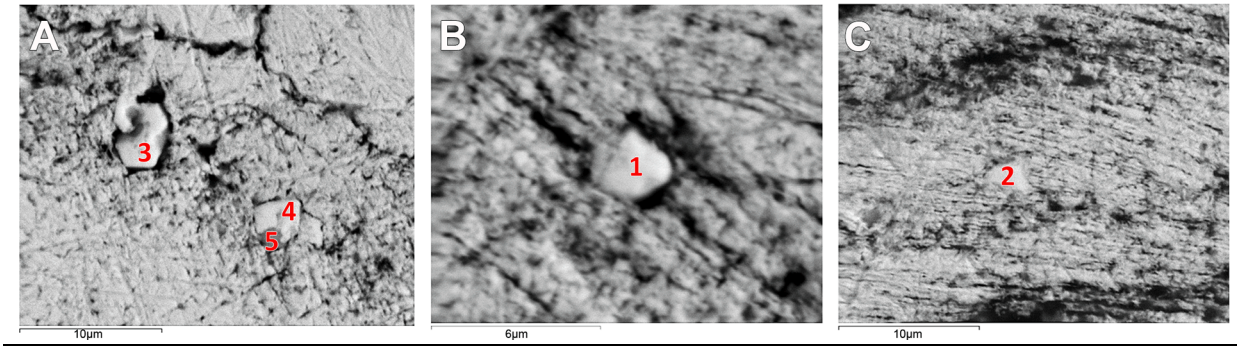

Table 5
Pb isotope ratios for MFA 47.1702 B2P1.

MFA Sample	$^{206}Pb/^{204}Pb$ (2 σ error)	$^{207}Pb/^{204}Pb$ (2 σ error)	$^{208}Pb/^{204}Pb$ (2 σ error)
47.1702 B2P1	18.8816 ± 0.0009	15.6766 ± 0.0009	38.8939 ± 0.0025

by spongy regions which are partly corroded ("B") and more extensively corroded, porous regions ("C"). The latter are mainly responsible for the dark layers visible in the back-scattered electron images. Some metal corrosion products are present, particularly in "C" regions. Notable throughout the section are very small angular grains (red arrows point to three of these in Fig. 3B). These were evidently harder than the surrounding metal, judging from how they behaved during polishing. Their compositions are discussed further below. At the surface ("S") are grains of metal isolated by extensive intergranular corrosion.

Analyses across the traverse indicate that the metal is an alloy of Ag with an Au content that averages a little <10 wt%. The original alloy composition is probably best represented by analyses of the uncorroded 'islands' (such as those labelled "A" in Fig. 3B). Analyses of various islands throughout the section indicate Au concentrations of 6–10%. This implies that the original alloy was probably not entirely uniform in composition. In Fig. 3D, differences in Ag and Au contents across the entire thickness of the section in one region are shown. Here, an uncorroded island included in the region analysed contained 6–7% Au. Notably, the Au content of regions of spongy and corroded regions is higher (10–12%) than in uncorroded islands. This is expected, as corrosion of the alloy would preferentially oxidise Ag allowing it to be removed through leaching, enriching the remaining metal in Au.

Table 3 presents analyses of 18 ~ 100 × 100 μm regions that extended over the entire section. The average Au content of these regions (which included islands and corroded regions) was 7%, which reflects the average Au content of the original alloy. The alloy also contains around 1% Cu. A small amount of Pb, typically <0.5%, is probably also present.

Inclusions may be variable in composition, but six analyses of them (Table 4) show that Pb and Sb are always major elements, probably with Ag and small amounts of other elements which include Fe and nickel (Ni). Because of their small sizes, the analyses probably include some of the surrounding Ag alloy. The inclusions also contain oxygen, so they may be oxides. Inclusion 5 was associated with another material of entirely different composition (Table 4) that is rich in Fe, Ni, Cu and Zn. These inclusions may be residual minerals associated with the silver ore deposit. They seem to have undergone little reaction during processing of the metal and forming and shaping of the object. That the bulk of micro-XRF measurements do not reveal quantifiable amounts of Sb indicates that these inclusions form only a small proportion of the mass of the bracelets. X-ray diffractometry shows that the corrosion products consist of Ag, with AgCl formed through chemical weathering of the Ag in a chloride-rich, salty environment. Further diffractometry on selected small pieces may help to reveal the mineralogy of these inclusions, as well as the bulk sample.

The Pb isotope composition of a sample from MFA 47.1702 B2P1 (Table 5) was compared with those from a galena (PbS) database including some 7000 localities located between the Atlantic Ocean and Iran. Lead isotope data on copper ores (Rademakers et al. 2021) have not been included, since; (1) the genesis of silver (felsic magmas) and copper ores (porphyry coppers) are very different, (2) the presence of an eutectic minimum makes extraction of silver from copper ores very challenging, and (3) Pb is essentially insoluble in copper.

The plots of Fig. 4 show the large scatter due to mass-dependent isotope fractionation, with possible causes being instrumental bias, incomplete yield during lead purification, or low-temperature weathering (Albarède et al., 2020). The slopes of the streaks in the binary plots (see also Artioli et al., 2020) are mass-dependent. They reveal mass-dependent isotope fractionation largely due to legacy (pre-2000) data in databases such as OXALID. The ellipses in Fig. 4 show the expected spread of isotopic data due to mass-dependent isotope fractionation. Both Euclidian distances (Delile et al., 2014; Birch et al., 2020) or, as in Fig. 5, distances to mass-dependent fractionation lines, a still unpublished special method dedicated to provenance search, give robust and consistent results. Although similarities in Pb isotope composition occur in unlikely sources such as Samos and Tunisia, which are not known for

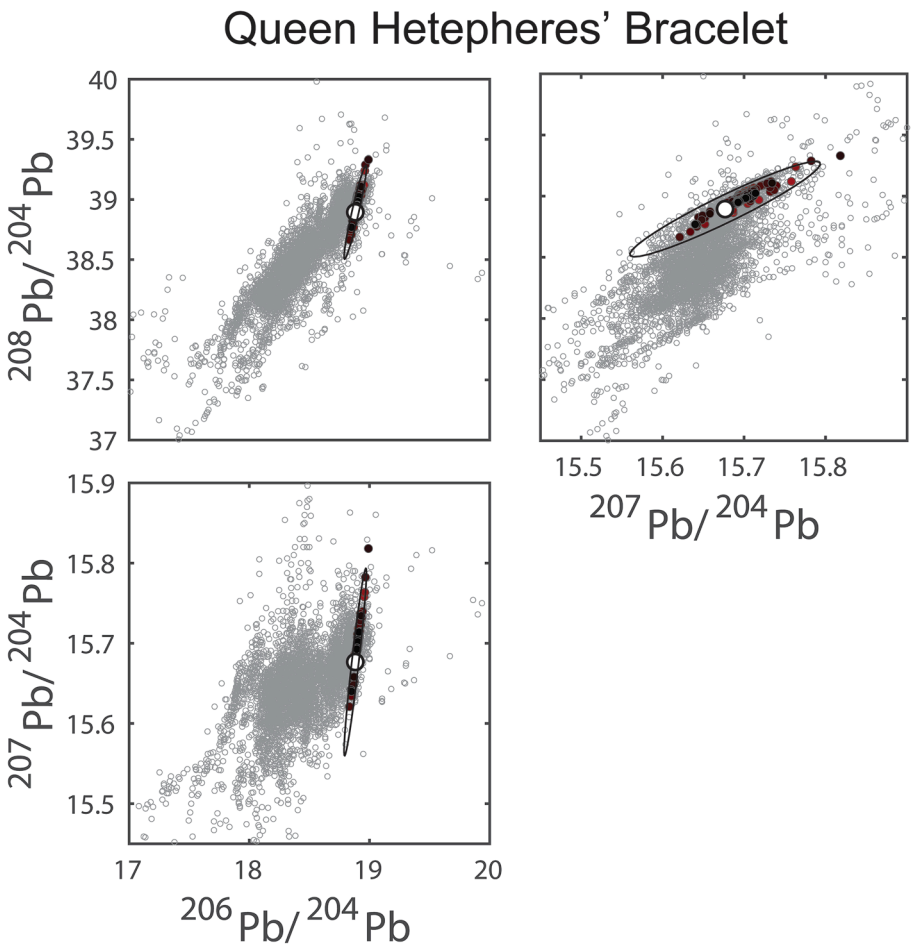

Fig 4. Lead isotope plots of 128 galena ores (on a black-to-yellow scale out of 7000, in grey) which are the closest to the MFA 47.1702 B2P1 sample (white circle) in the three-dimensional space of Pb isotope compositions. The ellipses represent the correlation caused by mass-dependent isotope fractionation for which possible causes are instrumental bias, incomplete yield during purification, or low-temperature weathering.

Ag production, the most significant 'hits' are from the Cyclades (Seriphos, which has more hits, Anafi, and Kea-Kithnos) (Fig. 5), and to a lesser from the Lavrion mines (district of Attica in central Greece). Anatolia, which has been suggested for the origin of Bronze Age copper-alloy artefacts on multiple occasions (see a discussion in Rademakers et al., 2021) can be, in the limits of ore data availability, excluded from consideration as a source.

Fig. 4 shows in conventional ^{204}Pb-normalized plots the 128 samples which are closest to the MFA 47.1702 B2P1 sample in the space of the three Pb isotope ratios. This finding is consistent with the results on Pb isotopes in *Hacksilber* from the Late Bronze and Iron Ages (Gentelli et al., 2021). This suggests that Aegean Ag, especially from the southern Aegean – known to have Ag production from Neolithic times (Nazou, 2020) and in the Early Bronze Age (Spitaels, 1984) at Thorikos – started spreading during the Bronze Age around the Mediterranean. The Cycladic islands are known Ag sources albeit with relatively small production. The Lavrion mines were much more productive in later times (Vaxevanopoulos et al., 2022) but provide a less compelling isotopic fit.

6. The historical setting

Lucas (1962) reported a high Au content of 8.9% for the bracelets which he suggested derived from aurian Ag (Ag which occurs occasionally in Au deposits) or from electrum, the *nbw ḥḏ* 'white gold' of early Egyptian inscriptions (Gale and Stos-Gale, 1981: 113). The possible use of aurian Ag was also suggested from analyses conducted on 33 Ag objects from Egypt dating from the Predynastic Period to Roman times albeit with considerable reservation (Gale and Stos-Gale, 1981: 111-112). With greater instrument precision and larger regional reference datasets now available, further clarity is now possible on the question of silver origins and exchange in the region.

Historical sources indicate that Ag was imported into Egypt during the Old Kingdom. The Royal Annals record under 4th Dynasty king Sneferu (date of reign c. 2613–2589 BC) '…silver and lapis lazuli…' in the context of imported commodities but the origins are not preserved (Strudwick, 2005: 66, S 235 (1) W 233). A late 6th Dynasty inscription (c. 2300 BC) lists Ag imported via the trade entrepôt of Byblos in Lebanon (Marcolin and Diego Espinel, 2011; Calligaro et al., 2014). By this time, Ag also passed through the city-state polity of Ebla in western Syria, from which it was exchanged as a commodity and a currency. Egypt enjoyed connections with Eblaite elites directly, through the mediation of Byblite agents, and through direct visitation of Eblaite representatives and regional commercial merchants to Egypt (Scandone Matthiae, 1981; Bevan, 2007; Sowada, 2009; Biga, 2012; Biga and Steinkeller, 2021). Silver is even specifically mentioned in the Ebla Texts as having been exchanged with Egypt (Biga and Steinkeller, 2021). The Ebla Texts also reveal that its elites had direct access to Ag mining in the Taurus Mountains (the ancient 'Silver Mountain') of Cilicia and sources in southeastern Anatolia (Scandone Matthiae, 1994; Winters, 2019; Massa, 2016; Biga and Steinkeller, 2021).

Yet during the time of king Sneferu, 300 years earlier than the 6th Dynasty, in-context material for Egyptian engagement with this region is not directly evident (Scandone Matthiae, 1979, 1981; Biga and Steinkeller, 2021). That said, Ebla may have begun exploiting regional Ag

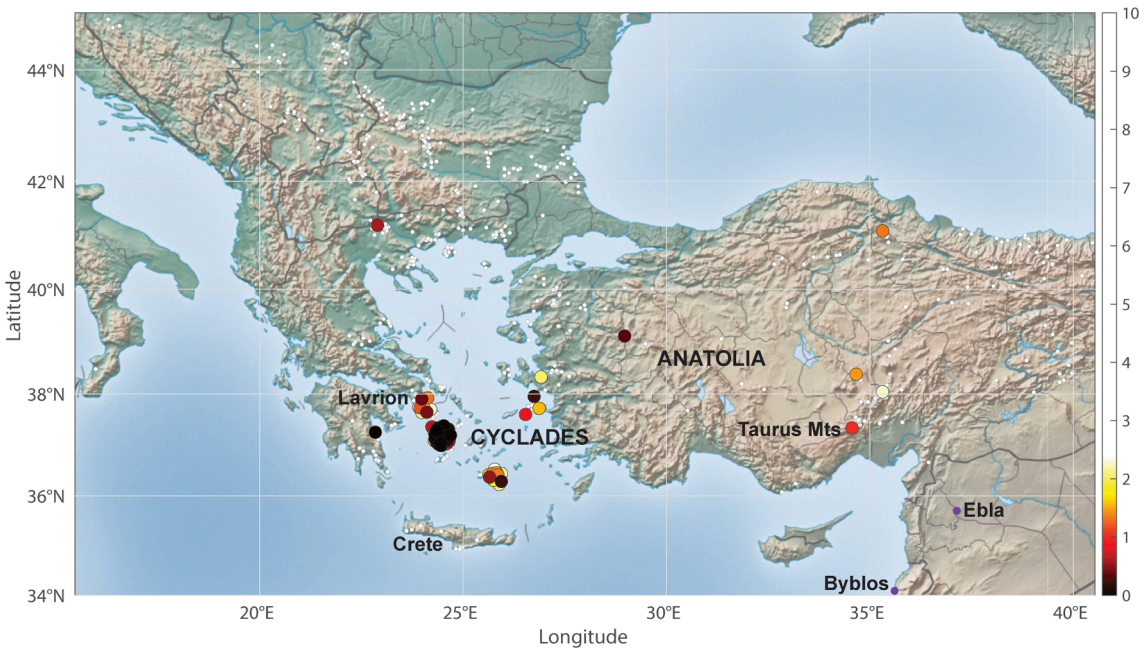

Fig 5. Map of the north-east Mediterranean and western Asia, showing potential silver sources (Source F. Albarède). The Pb isotope composition of a sample from MFA 47.1702 B2P1 is compared with the compositions of nearly 7000 samples of galena (white dots) distributed from the Atlantic Ocean to the Indian Ocean from the Ecole Normale Supérieure de Lyon database. The distance (color bar to the right) allows 128 galena samples with the closest Pb isotope compositions relative to MFA 47.1702 B2P1 to be retained. Unlikely sources can be ignored. A black symbol color indicates a high probability of provenance with the greatest density of 'hits' coming from Seriphos, Anafi, and Kea-Kithnos in the Cyclades, and to a lesser degree Lavrion. Red and orange symbols indicate less probable sources (Anatolia, Macedonia). The symbol sizes have been slightly jittered and enlarged to increase visibility of the less probable points.

sources at an early time, with the metal acquired by Egypt through Byblos. Alternatively, the Egyptian state could have engaged directly with the Taurus region, as suggested by a unique jug from Cilicia in an early 4th Dynasty tomb (Sowada, 2009: MFA 20.1904, 71[55] and references). Importantly, a shift in silver exchange networks from the Aegean to western Anatolia over this long chronological horizon is also possible; Ag sources in the Aegean were worked in the fourth and third millennium (Maran, 2021). By 2300 BC, both networks may have operated, but further evidence is needed.

Lead isotope ratios of B2P1 are closest to values consistent with Ag mined in the Cycladic islands in the Aegean and to a lesser extent with the Lavrion mines (Vaxevanopoulos et al., 2022). Anatolia (Western Asia) is an unlikely source. This finding exposes the likelihood of previously unattested direct or indirect exchange between Egypt and the Aegean at this early period. Speculation on this relationship has persisted for decades based on third millennium BC Egyptian stone vessels and other objects found in Early Minoan Crete (Bevan, 2007; Phillips, 1996, 2008; Sowada, 2009). As Maran (2021) demonstrates, Lavrion sources were exploited not only during the third millennium BC, but also during the Aegean Chalcolithic era of the 4th millennium BC, with concomitant metallurgical practice and innovation. The possible extent of Aegean Ag exploitation and exchange thus provides a context for the presence of Ag objects at *énéolithique* Byblos c. 3800–3200 BC (Prag, 1978). The proposition of Aegean Ag circulating in the eastern Mediterranean at this early time raises significant questions about the complexity of social and economic interactions across the region that requires further analytical study.

7. Conclusions

The results of multi-proxy analysis on fragments from the bracelets of queen Hetepheres I identified the metal as silver. Egypt has no local sources of this metal, but it was likely locally alloyed with an original content of average 7% gold to improve its malleability and appearance when worked. For the first time, SEM images reveal the methods of early Egyptian silverworking; the bracelets were made by hammering cold-worked metal, with frequent annealing to prevent breakage.

Lead isotope analysis indicates that the silver was most likely obtained from the Cyclades (Seriphos, Anafi, or Kea-Kithnos) or perhaps the Lavrion mines in Attica. It excludes Anatolia as the source with a fair degree of certainty. This new finding demonstrates, for the first time, the potential geographical extent of commodity procurement networks utilized by the Egyptian state during the early Old Kingdom at the height of the Pyramid-building age.

Credit authorship contribution statement

Karin Sowada: Conceptualization, Methodology, Writing – original draft, Writing – review & editing, Visualization, Supervision. **Richard Newman:** Methodology, Validation, Formal analysis, Investigation, Resources, Data curation, Writing – original draft, Writing – review & editing, Visualization. **Francis Albarède:** Validation, Formal analysis, Resources, Writing – original draft, Writing – review & editing, Visualization, Supervision. **Gillan Davis:** Conceptualization, Writing – original draft, Writing – review & editing. **Michele R. Derrick:** Investigation. **Timothy D. Murphy:** Investigation, Data curation, Visualization. **Damian B. Gore:** Methodology, Validation, Formal analysis, Investigation, Resources, Data curation, Writing – original draft, Writing – review & editing, Visualization, Supervision.

Declaration of Competing Interest

The authors declare that they have no known competing financial interests or personal relationships that could have appeared to influence the work reported in this paper.

Acknowledgements

We thank the Museum of Fine Arts, Boston, for permission to study and sample the bracelets. In particular, the Head of the Department of

Ancient Art Dr Rita Freed and Curator Dr Denise Doxey provided every support for the on-site work. We thank Marine Pinto and Janne Blichert-Toft (both École normale supérieure de Lyon) for lead isotope analyses, and Alice McClymont, Dr Anna-Latifa Mourad and Nathaniel Lowe (Macquarie University) for assistance with the illustrations. We are indebted to the Macquarie University Centre for Ancient Cultural Heritage and Environment (CACHE) for its support.

Funding source

This work was supported by the Australian Research Council Future Fellowship Grant FT170100288 held by Karin Sowada. Francis Albarède acknowledges support from the H2020 European Research Council Advanced Grant Number 741454-SILVER-ERC-2016-ADG.

Appendix A. Supplementary data

Supplementary data to this article can be found online at https://doi.org/10.1016/j.jasrep.2023.103978.

References

Albarède, F., Blichert-Toft, J., Gentelli, L., Milot, J., Vaxevanopoulos, M., Klein, S., Westner, K., Birch, T., Davis, G., de Callataÿ, F., 2020. A miner's perspective on Pb isotope provenances in the Western and Central Mediterranean. J. Archaeol. Sci. 121, 105194.

Aldred, C., 1971. Jewels of the Pharaohs. Thames and Hudson, New York.

Artioli, G., Canovaro, C., Nimis, P., Angelini, I., 2020. LIA of prehistoric metals in the Central Mediterranean area: a review. Archaeometry 62, 53–85.

Bevan, A., 2007. Stone Vessels and Values in the Bronze Age Mediterranean. Cambridge University Press, New York.

Biga, M., 2012. Tra Egitto e Siria nel III millennio a.C. Atti dell' Accademia delle Scienze di Torino, Classe di Scienze Morale, Storiche e Filologische 146, 17–36.

Biga, M., Steinkeller, P., 2021. In Search of Dugurasu. J. Cuneiform Stud. 73, 9–70. https://doi.org/10.1086/114822.

Birch, T., Westner, K., Kemmers, F., Klein, S., Höfer, H.E., Seitz, H.M., 2020. Retracing Magna Graecia's silver: coupling lead isotopes with a multi-standard trace element procedure. Archaeometry 62, 81–108.

Calligaro, T., Coquinot, Y., Pichon, L., Pierrat-Bonnefois, G., de Campos, P., Re, A., Angelici, D., 2014. Characterization of the lapis lazuli from the Egyptian treasure of Tôd and its alteration using external μ-PIXE and μ-IBIL. Nucl. Instrum. Methods Phys. Res., Sect. B 318, Part A, 139–144. https://doi.org/10.1016/j.nimb.2013.06.063.

Delile, H., Blichert-Toft, J., Goiran, J.-P., Keay, S., Albarède, F., 2014. Lead in ancient Rome's city waters. Proc. Natl. Acad. Sci. 111, 6594–6599.

Gale, N.H., Stos-Gale, Z.A., 1981. Ancient Egyptian silver. J. Egypt. Archaeol. 67, 103–115. https://doi.org/10.2307/3856605.

Gentelli, L., Blichert-Toft, J., Davis, G., Gitler, H., Albarède, F., 2021. Metal Provenance of Iron Age Hacksilber hoards in the southern Levant. J. Archaeol. Sci. 134, 105472 https://doi.org/10.1016/j.jas.2021.105472.

Hartung, U., Köhler, E.C., Müller, V., Ownby, M., 2015. Imported pottery from Abydos: a new petrographic perspective. Ägypten und Levante 25, 293–333.

Hartung, U. 2001. Umm el-Qaab II. Importkeramik aus dem Friedhof U in Abydos (Umm el-Qaab) und die Beziehungen Ägyptens zu Vorderasien im 4. Jahrtausend v. Chr. Archäologische Veröffentlichungen, Deutsches Archäologisches Institut, Abteilung Kairo 92. Mainz: Philipp von Zabern.

Harvard, 2023. Digital Giza. The Giza Project at Harvard University. Accessed April 2023. http://giza.fas.harvard.edu.

Hauptmann, A., von Bohlen, A., 2011. Aurian silver and silver beads from tombs at el-Mahâsna, Egypt. In: Friedman, R.F., Fiske, P.N. (Eds.), Egypt at its Origins 3. Proceedings of the Third International Conference "Origin of the State. Predynastic and Early Dynastic Egypt", London, 27th July–1st August 2008. Peeters: Leuven/Paris/Walpole, MA, pp. 430–435.

Kmošek, J., Odler, M., Fickle, M., Kochergina, Y.V., 2018. Invisible connections. Early Dynastic and Old Kingdom Egyptian metalwork in the Egyptian Museum of Leipzig University. JOAS 96, 191–207. https://doi.org/10.1016/j.jas.2018.04.004.

Lucas, A., Harris, J.R., 1962. Ancient Egyptian Materials and Industries, 4th ed. 1989 reprint by Histories & Mysteries of Man, London.

Maran, J., 2021. Attica and the Origins of Silver Metallurgy in the Aegean and the Carpatho-Balkan Zone. In: Kalogeropoulos, K., Vassilikou, D., Tiverios., M., . (Eds.), Sidelights on Greek Antiquity. Archaeological and Epigraphical Essays in Honour of Vasileios Petrakos. De Gruyter:, Berlin, pp. 197–225.

Marcolin, M., Diego Espinel, A., 2011. The Sixth Dynasty biographic inscriptions of Iny: More pieces to the puzzle. In: Bárta, M., Coppens, F., Krejcí, J. (Eds.), Abusir and Saqqara in the year 2010/1. Czech Institute of Egyptology, Prague, pp. 570–615.

Massa, M., 2016. Networks before Empires: cultural transfers in western and central Anatolia during the Early Bronze Age. University College London. Doctoral Dissertation.

Milot, J., Malod-Dognin, C., Blichert-Toft, J., Télouk, P., Albarède, F., 2021. Sampling and combined Pb and Ag isotopic analysis of ancient silver coins and ores. Chem. Geol. 564, 120028 https://doi.org/10.1016/j.chemgeo.2020.120028.

Mishara, J., Meyers, P. 1974. Ancient Egyptian silver: a review, in: Bishay, A. (Ed.), Recent Advances in Science and Technology of Materials: Proceedings of the Cairo Solid State Conference 3. Plenum Press, New York, pp. 29–45.

Nazou, M., 2020. Just a long boat ride away: Maritime interaction in the southern Aegean Sea during the Final Neolithic period. Shima 14 (1), 152–171.

Ogden, J., 2000. Metals. In: Nicholson, P.T., Shaw, I. (Eds.), Ancient Egyptian Materials and Technology. Cambridge University Press, Cambridge, pp. 148–176.

Ownby, M.F., Hartung, U., Sowada, K., 2022. The jars from Tomb U-j – a petrographic and contextual re-assessment. Ägypten und Levante 32, 231–268. https://austriaca.at/?arp=0x003df239.

Petrie, W.M.F. 1901. Royal Tombs of the Earliest Dynasties. Memoir 21. Egypt Exploration Fund, London.

Phillips, J., 2008. Aegyptiaca on the Island of Crete in Their Chronological Context: A Critical Review, Volume I-II. Verlag der Österreichischen Akademie der Wissenschaften:, Vienna.

Phillips, J., 1996. 'Aegypto-Aegean Relations up to the 2nd millennium BC'. In: Krzyzaniak, L., Kroeper, K., Kobusiewicz, M. (Eds.), Interregional Contacts in the later Prehistory of Northeastern Africa (Poznan). pp. 459–470.

Prag, K., 1986. Byblos and Egypt in the Fourth Millennium BC. Levant 18, 59–74. https://doi.org/10.1179/lev.1986.18.1.59.

Prag, K., 1978. Silver in the Levant in the Fourth Millennium B.C. In: Piotrovsky, B.B. (Ed.), Archaeology in the Levant: Essays for Kathleen Kenyon. Aris & Phillips, Warminster, pp. 36–45.

Rademakers, F.W., Verly, G., Delvaux, L., Degryse, P., 2021. Provenance reinterpretation of some early Egyptian copper alloy artefacts. J. Archaeol. Sci. Rep. 38, 103095.

Reisner, G.A., 1927. Hetep-heres, mother of Cheops. Museum Fine Arts Bull. 25 (Supplement), 1–36.

Reisner, G.A., 1928. Silver in ancient times. J. Egypt. Archaeol. 14 (3–4), 313–319.

Reisner, G.A., Smith, W.S., 1955. The History of the Giza Necropolis. Volume II: The Tomb of Hetep-heres the Mother of Cheops. A Study of Egyptian Civilization in the Old Kingdom. Harvard University Press, Cambridge, MA.

Scandone Matthiae, G., 1979. Vasi inscritti di Chephren e Pepi I nel Palazzo Reale G di Ebla. SEb 1, 33–43.

Scandone Matthiae, G., 1981. I Vasi Egiziani in Pietra del Palazzo Reale G, SEb 4, 99–127.

Scandone Matthiae, G. 1994. La cultura egiziana a Biblio attraverso le testimonianze materiali. In: Acquaro E., Mazza, F., Ribichini, S., Scandone, G., Xella, P. (Eds.), Biblio. Una città e la sua cultura. Atti del Colloquio Internazionale, Roma, 5-7 dicembre 1990 (Collezione di Studi Fenici 34, Rome), pp. 37–48.

Shaw, I., 2000. Chronology. In: Shaw, I. (Ed.), The Oxford History of Ancient Egypt. Oxford University Press, Oxford/New York, pp. 480–489.

Sowada, K., 2009. Egypt in the Eastern Mediterranean during the Old Kingdom: An Archaeological Perspective. Orbis Biblicus et Orientalis 237. Academic Press/Vandenhoeck and Ruprecht, Fribourg. https://doi.org/10.5167/uzh-143040.

Spitaels, P., 1984. The Early Helladic Period in Mine no 3 (Theatre Sector), in: Thorikos VIII (1972–76), Rapport preliminaire sur les 9,10,11 and 12, campagnes de fouilles. Comité des fouilles Belges en Grèce, pp. 151–174.

Strudwick, N., 2005. Texts from the Pyramid Age. Society of Biblical Literature, Atlanta.

Vaxevanopoulos, M., Blichert-Toft, J., Davis, G., Albarède, F., 2022. New findings of Ancient Greek silver sources. J. Archaeol. Sci. 137, 105474. https://doi.org/10.1016/j.jas.2021.105474.

Winters, R.D., 2019. Negotiating Exchange: Ebla and the International System of the Early Bronze Age. Harvard University, Graduate School of Arts & Sciences. Doctoral dissertation,.

Ziegler, C., 1999. L'art égyptien au temps des pyramides. Réunion des Musées Nationaux, Paris.